

Geochemistry of the rare-earth elements and uranium in the acidic Berkeley Pit lake, Butte, Montana

Christopher H. Gammons^{a,*}, Scott A. Wood^b, James P. Jonas^c, James P. Madison^d

^aDepartment of Geological Engineering, Montana Tech of The University of Montana, 1300 West Park St., Butte, MT 59701, USA

^bDepartment of Geological Sciences, University of Idaho, Moscow, ID 83844-3022, USA

^cCDM Federal Programs Corporation, Denver, CO 80202, USA

^dMontana Bureau of Mines and Geology, Montana Tech of The University of Montana, Butte, MT 59701, USA

Received 16 April 2002; accepted 28 December 2002

Abstract

Filtered (0.45 μm) and nonfiltered concentrations of rare-earth elements (REE), U, Zr, Th, Ba, Sc, and Y were measured as a function of depth in the Berkeley Pit lake, a large acidic mining lake in Butte, MT. The REE show very little variation with depth, apart from a slight concentration near the surface, presumably due to evaporation. The REE profiles of the pit waters show a depletion in light REE when normalized against NASC and the host Butte Quartz Monzonite (BQM), and a possible enrichment in middle REE vs. heavy REE when normalized against BQM. All of the REE partitioned weakly into secondary ferric precipitates formed by aging of deep Berkeley Pit water. The measured distribution coefficients increased across the lanthanide series from La ($K_d = 7.7$) to Nd ($K_d = 10.3$), and then decreased steadily to Lu ($K_d = 1.4$). Under the conditions of the Berkeley Pit lake, the aqueous speciation of REE and U is dominated by sulfate complexes. Because the stability constants of REE–sulfate complexes show very little variation across the lanthanide series, the observed trends in K_d cannot be explained by aqueous complexation. Despite high concentrations of dissolved REE (e.g., 1.1 mg/l Ce) and U (0.85 mg/l), saturation indices for all solid phases were strongly negative, due to the low pH of the Berkeley Pit lake (2.3–2.6). The mobility of REE and U is more likely constrained by adsorption or co-precipitation with strengite, jarosite, schwertmannite, or other secondary minerals forming in the lake.

© 2003 Elsevier Science B.V. All rights reserved.

Keywords: Rare-earth elements; Geochemistry; Acid rock drainage; Uranium; Pit lake

1. Introduction

The rare-earth elements (REE) have been increasingly applied as tracers of geochemical processes

in natural waters such as seawater, lake water, river water, and groundwater (see, for example, Sholkovitz and Schneider, 1991; Sholkovitz, 1992; Johannesson and Lyons, 1994, 1995; German et al., 1995; Johannesson and Hendry, 2000). Recent attention has focused specifically on the behavior of REE in acidic waters (Carlson-Foszcz et al., 1991; Miekeley et al., 1992; Webb et al., 1993; Nordstrom et al., 1995; Gimeno et al., 1996, 2000;

* Corresponding author. Tel.: +1-406-496-4763; fax: +1-406-496-4260.

E-mail address: cgammons@mtech.edu (C.H. Gammons).

Verplanck et al., 1997, 1998a,b, 1999; Leybourne et al., 1998, 2000; Pearce et al., 1998; White et al., 1998; Elbaz-Poulichet and Dupuy, 1999; Hollings et al., 1999; Åström, 2001; Worrall and Pearson, 2001a,b; Wood et al., in press). Most of the waters in question gained their acidity by weathering of sulfide minerals, through natural or anthropogenic processes. The ultimate goal of these studies is to use the REE as a tool to better understand geochemical processes during acid rock drainage (ARD) formation and subsequent mobilization of heavy metals. However, many aspects of REE geochemistry in acidic waters remain poorly understood.

To enhance the current understanding of the behavior of REE in acid drainage, we have determined the concentrations of these elements, as well as uranium, in the acidic Berkeley Pit lake. To our knowledge, these are the first REE data reported from a flooded open-pit mine. The results are discussed and placed within the context of previous studies of REE in acidic waters.

2. Background

The Berkeley Pit lake, located in Butte, MT (Fig. 1), is one of the largest and most highly publicized mining pit lakes in the world. The Berkeley open pit operated from 1953 to 1982, mining the central, copper-rich portion of a very large, polymetallic, porphyry–epithermal system (Meyer et al., 1968; Miller, 1973). The host rock of the deposit is a highly altered granite locally known as the Butte Quartz Monzonite (BQM). Approximately 320 million tons of ore and >700 million tons of waste rock were removed from the pit. In addition, more than 10,000 km of underground tunnels, shafts, and stopes were mined in the Butte district in the 110-year period from 1870 to 1980. The interconnected underground workings extend to a depth of >1500 m, and are spread over a 20-km² area (Fig. 1). The Berkeley Pit lake began forming in 1983, shortly after mining of the open pit ceased and dewatering pumps were turned off. Since 1983, the lake has served as a sump, collecting polluted groundwater from the surrounding

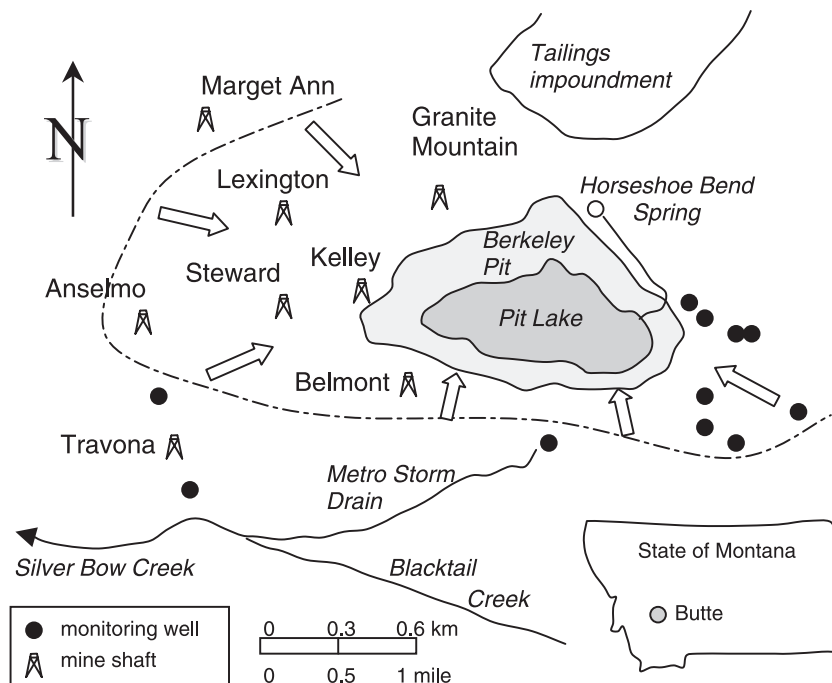


Fig. 1. Map of Butte, MT, showing the location of the Berkeley Pit, Yankee Doodle tailings pond, and Horseshoe Bend spring, as well as selected shafts and bedrock monitoring wells. The dashed line shows the approximate drainage divide between groundwater heading towards the Berkeley Pit (arrows), and groundwater that ultimately discharges to the Metro Storm Drain or Silver Bow Creek.

bedrock and flooded underground mine workings (Duaiame et al., 1998; Metesh and Duaiame, 2000). Flooding continues to this day at a rate of 3–5 million gallons/day ($11\text{--}19 \times 10^6$ l/day).

As of December 2001, the lake was 220 m deep at its center, and contained over 31 billion gallons ($>1.11 \times 10^{11}$ l) of acidic and metal-rich mine water. The aqueous geochemistry of the Berkeley Pit lake has been summarized elsewhere (Davis and Ashenberg, 1989; Robins et al., 1997; Jonas, 2000; Gammons et al., in review). The lake is strongly acidic (15-year mean pH=2.63), and is extremely enriched in heavy metals, including iron (>800 mg/l), zinc (600 mg/l), and copper (150–200 mg/l). A representative analysis of Berkeley Pit water, collected in May of 1998 at a depth of 15.2 m below surface, is given in Table 1.

For the majority of the year, the Berkeley Pit lake has a distinct thermocline located roughly 3–15 m below surface, separating the deep hypolimnion from the shallow and more oxidized epilimnion (Jonas, 2000). Changes in the chemistry of the lake with depth were summarized by Jonas (2000) and Gammons et al. (in review). The most prominent feature with respect to the lake's chemical limnology is a transition from ferrous-rich water at depth to ferric-rich water near the surface. The concentration of total iron is lower above the thermocline, due to oxidation of Fe^{2+} to Fe^{3+} , and the subsequent formation of secondary ferric precipitates. These precipitates scavenge certain trace elements, including arsenic, boron, potassium, and phosphorus (Jonas, 2000).

In the first 12 years of mine flooding, a large acidic spring—known as the Horseshoe Bend spring—was a

major input in the overall water budget of the Berkeley Pit lake. Between 1996 and 2000, the Horseshoe Bend spring was diverted away from the pit, treated with lime, and discharged into a nearby tailings impoundment (Fig. 1). This decreased the flooding rate of the Berkeley Pit from 19×10^6 to 11×10^6 l/day (Duaiame et al., 1998). From June 2000 to the present day, the Horseshoe Bend discharge has again been diverted into the pit. The collection of all samples and analytical data in this study took place in 1998 and 1999, during the period when the Horseshoe Bend spring was diverted away from the pit. During this time, the geochemistry of the lake was dominated by groundwater inputs, water–rock interaction along the submerged mine walls, and internal metal cycling (Gammons et al., in review). For further information on issues regarding monitoring and management of the Berkeley Pit lake, the interested reader is referred to www.pitwatch.org.

Chemical analyses of water samples collected from the Berkeley Pit lake between 1982 and 2000 have recently been compiled by Metesh and Duaiame (2000). Despite this wealth of information, no previous data have been reported on the REE or U concentrations of the Berkeley Pit lake.

3. Methods

3.1. Sample collection

Samples of Berkeley Pit water for REE and U analysis were collected on July 1, 1999, by Montana Bureau of Mines and Geology (MBMG) personnel, using the MBMG research boat, which is permanently stationed on the pit lake. Samples were collected at depths of 0.3, 0.91, 1.52, 3.05, 9.14, 15.2, 30.5, 91.4, 152.4, and 210 m below the lake surface, the last sample being 3 m above the lake bottom at the point of sampling. Samples at 91.4, 152.4, and 210 m were taken with a General Oceanics Model 1080 series GO-FLO PVC water sampling bottle supported from a graduated nylon rope. For depths ≤ 30 m, samples were collected with a peristaltic pump and flexible 5/16-in. (0.79 cm) Teflon tubing. At least 4 l of water (3 tube volumes at 30 m depth) was pumped and discarded before each sample was collected. The tubing was taped to a cable supporting a submersible water-

Table 1
Bulk composition of Berkeley Pit water^a

| Component | mg/l | Component | mg/l |
|---------------------|------|------------------|------|
| SO_4^{2-} | 9150 | Cu^{2+} | 196 |
| Fe^{2+} | 778 | Na^+ | 105 |
| Zn^{2+} | 645 | Si^{4+} | 54 |
| Mg^{2+} | 504 | F^- | 32 |
| Ca^{2+} | 465 | DIC ^b | 21.3 |
| Fe^{3+} | 329 | Cl^- | 12 |
| Al^{3+} | 300 | K^+ | 9.4 |
| Mn^{2+} | 231 | P^{5+} | 0.72 |
| $T=4.2$ °C, pH=2.54 | | VO_2^+ | 0.36 |

^a Sampled in May 1998 from depth of 15 m below surface (Jonas, 2000).

^b Dissolved inorganic carbon (mg C/l).

quality multiprobe, and depth was measured using calibrations on the cable. Although the multiprobe malfunctioned on this particular sampling day, a set of water-quality field parameters was collected 8 days later (see below). Prior to leaving for the field, 2 ml of Trace-Metal Grade, concentrated HCl was added to 120-ml, opaque, HDPE sample bottles. At each depth, both a filtered and nonfiltered sample were taken. The nonfiltered sample was transferred from either the peristaltic pump or the GO-FLO sampling bottle directly to the 120-ml sample bottle. Water for the filtered sample was temporarily stored in a 250-ml HDPE beaker (rinsed three times with deionized water followed by three times with pit water). This water was then sampled with a 50-cm³ polypropylene syringe (rinsed three times with deionized water followed by three times with pit water) and transferred through a 0.45- μ m cellulose acetate syringe filter into a 120-ml HDPE bottle, preloaded with 2 ml of HCl. After sampling, the bottles were capped and sealed tightly with Parafilm, and stored in a refrigerator. The analyses were completed within 6 months of sampling.

Because the samples collected in this study were only analyzed for REE and selected trace elements, it was necessary to combine these results with previous investigations to get a complete water chemistry profile. A comprehensive depth sampling of Berkeley Pit water was conducted in May of 1998 (Jonas, 2000), using the same procedures outlined above. These samples were analyzed for a complete suite of metals (ICP-AES), anions (IC), and total inorganic carbon, as well as Fe³⁺ and Fe²⁺. Additional details are given in Jonas (2000). In the May 1998 sampling, preliminary ICP results were obtained for selected REE, including La, Ce, and Nd. These early results indicated elevated levels (up to \sim 1 mg/l) of REE in the pit waters, and provided the impetus for the present investigation.

3.2. Field parameters

MBMG personnel collected a set of field parameters in the Berkeley Pit as a function of depth on July 9, 1999, 8 days after the samples for REE analysis were collected. A Hydrolab Data Sonde 3 water-quality multiprobe was lowered on a cable and output was logged on the vessel with a laptop computer. Parameters measured included pH, temperature, specific conductivity (SC), Eh, dissolved oxygen (DO), and

turbidity. The pH was calibrated with pH 2 and 7 buffers. Specific conductivity was calibrated with a 5000 μ S/cm KCl solution. The Eh was calibrated with a mixture of quinhydrone solution and pH 4 and 7 calibration standards. The quinhydrone and pH 4 and 7 buffers provide 462 and 285 mV reference Eh standards, respectively, at 25 °C. DO was calibrated to 100% saturation (7.7 mg/l) and zeroed with nitrogen gas. Turbidity was calibrated with 5 and 40 Nephelometric Turbidity Units (NTU) calibration solution.

3.3. REE analysis

The REE analyses of Berkeley Pit waters were performed by Dr. William Shannon, using an inductively coupled plasma-mass spectrometer (ICP-MS; Hewlett Packard model 4500) at Washington State University. The samples were diluted 10 times into a matrix of 4% HNO₃, 1% HCl, and were analyzed together with bracketing quality-control samples and matrix-matched standards. Oxide formation as measured by ¹⁵⁶CeO/¹⁴⁰Ce was typically less than 0.5%, equivalent to ²⁴⁸ThO/²³²Th of less than 1%. Corrections for isobaric oxide interferences were made for BaO on Eu and Sm, PrO on Gd, and NdO on Tb. Corrections were made by periodically running both a 10-mg/l Ba standard and a mixed Pr–Nd standard. Ruthenium, In, and Re were employed as internal standards. All data reduction was accomplished off-line using a standardized computer spreadsheet. No unusual problems were encountered during the analyses, and all of the REE concentrations obtained were orders of magnitude above the method detection limits. Analytical precision was estimated at \pm 2%. A procedural blank and two blind duplicate samples were included in the sample matrix. Concentrations of all analytes in the blank sample were less than 0.5% of their respective concentrations in Berkeley Pit water, with the exception of Ba and Zr, which had anomalously high blanks. The duplicate samples gave standard errors (1 σ /mean) of less than 0.5% for all analytes, with the exception of Zr (2.7%).

3.4. Partitioning experiments

Secondary precipitates are known to form in the upper portion of the Berkeley Pit lake, due to oxidation of ferrous to ferric iron. A bench-top partitioning

experiment was conducted to test whether the REE could fractionate during this process. Berkeley Pit water collected at 15 m depth was aged at room temperature on the bench top. The experiments were set up in three identical 1-l beakers, and covered with a watch glass. The samples did not receive direct sunlight, although no attempt was made to shield the samples from indirect sunlight or room light. A dark red precipitate formed in all containers within a few days. The first beaker was sampled after 15 days, the second after 30 days, and the third after 50 days. The mass of water in each container was measured before and after the experiment, to monitor evaporative loss of water. In each case, a filtered (0.45 μm) aqueous sample was taken and preserved to 2% HCl, and the precipitate was recovered by a combination of filtering and centrifugation. The precipitates were rinsed several times with deionized water and dried over-

night at 40 °C. After weighing, an aliquot of solid was dissolved in 5% HCl, and split into two subsamples. One set was analyzed for REE by ICP-MS, as described above for the water samples. The other set was analyzed for a conventional suite of major and trace elements by ICP-AES.

4. Results

4.1. Field parameters

Changes in field parameters (temperature, pH, turbidity, and Eh) with depth for the Berkeley Pit on July 9, 1999, are shown in Fig. 2. The temperature profile indicates a distinct thermocline at roughly 5 m depth, below which point the pit had a nearly constant temperature of 4–6 °C to the bottom of the

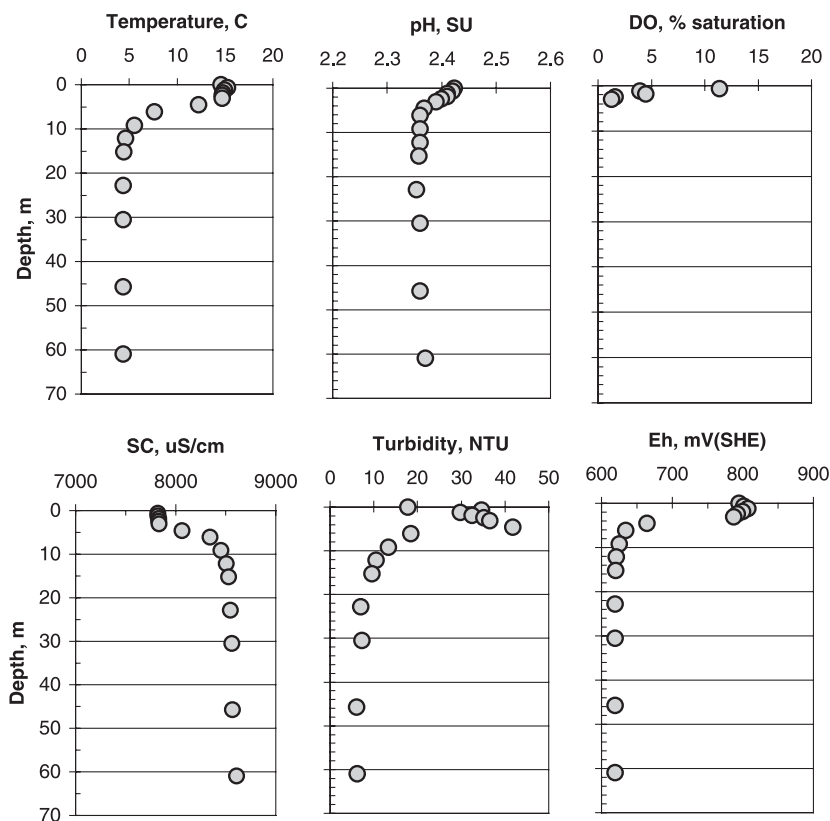
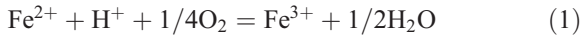


Fig. 2. Changes in field parameters vs. depth in the Berkeley Pit lake on July 9, 1999. Temperature is given in °C; pH in standard units (SU); dissolved oxygen (DO) in % of local atmospheric saturation; specific conductivity (SC) in $\mu\text{S}/\text{cm}$; turbidity in Nephelometric Turbidity Units (NTU); and Eh in mV, corrected to the Standard Hydrogen Electrode (SHE).

lake. The pH of the lake waters was <2.5 at all depths, and was slightly higher above the thermocline, most likely due to consumption of protons during oxidation of Fe^{2+} to Fe^{3+} (Gammons et al., *in review*), as shown by the following reaction:



Oxidation of Fe^{2+} lowered dissolved oxygen to undetectable levels in the top 2 m of the lake (Fig. 2). The measured Eh showed a sharp drop below the thermocline, coinciding with a shift in the dominant oxidation state of dissolved iron from the ferric to ferrous state (Jonas, 2000; Gammons et al., *in review*). Oxidation of Fe^{2+} to Fe^{3+} also resulted in supersaturation and precipitation of secondary ferric minerals, causing a significant decrease in total dissolved iron above the thermocline (Jonas, 2000). This is represented by an increase in turbidity and decrease in specific conductivity (SC) in the shallow lake (Fig. 2). SC was uniform below the thermocline, indicating the absence of any chemical stratification at depth. This is consistent with the lack of change in the concentration of major and trace elements (Jonas, 2000), which suggests that the lake below the thermocline is vertically well mixed.

4.2. REE trends in host rock

REE analyses for altered Butte Quartz Monzonite (BQM) samples were supplied by Mark Reed (University of Oregon), and were determined by Instrumental Neutron Activation Analysis (INAA). Although not all of the REE were analyzed in this earlier study, enough data are available to show general trends. As shown in Fig. 3, hydrothermally altered BQM is strongly enriched in LREE relative to C1 chondrite (Anders and Grevesse, 1989). A much flatter REE profile is obtained when the same rocks are normalized against North American Shale Composite (NASC; Gromet et al., 1984), although there are subtle differences depending on the style and intensity of alteration. Of the various BQM alteration facies included in Fig. 3, rock in the Berkeley Pit would be most closely represented by the “gray sericite” and “pale green sericite” samples. These two samples show especially flat trends in REE when normalized vs. NASC (Fig. 3b). The more weakly

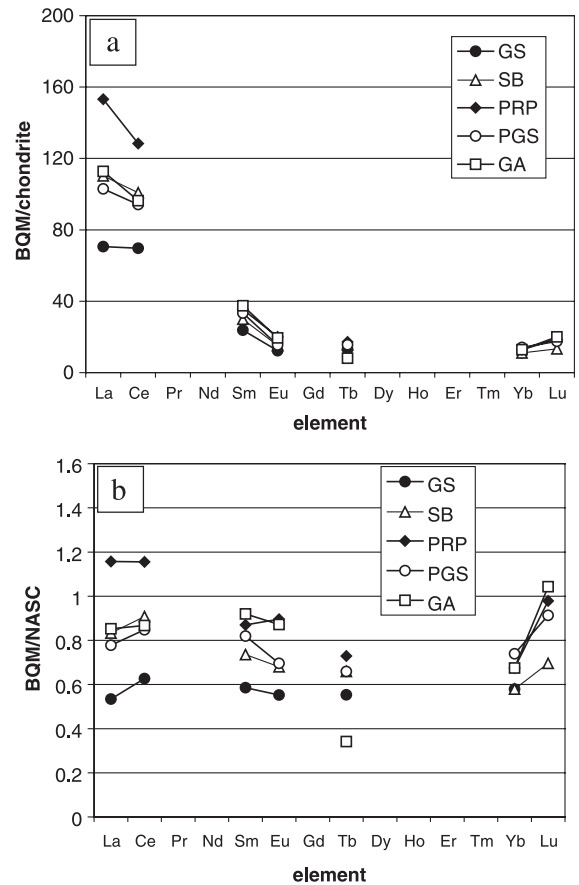


Fig. 3. REE profiles of hydrothermally altered Butte Quartz Monzonite (BQM), normalized to: (a) C1 chondrite; (b) North American Shale Composite (NASC). REE data for BQM were supplied by Mark Reed (University of Oregon). Abbreviations: GS=gray sericite; SB=sericite with remnant biotite; PRP=propylitic; PGS=pale green sericite; GA=green argillic.

altered “propylitic” and “argillic” samples show a depletion in middle REE vs. NASC. However, this type of relatively weak alteration is not present in the immediate vicinity of the Berkeley Pit.

A preliminary REE study of hydrothermal fluids in fluid inclusions from the Butte ore body was reported by Ghazi et al. (1994). These data showed a general enrichment in LREE when normalized to C1 chondrite, with negligible Ce or Eu anomalies. Fig. 3a shows that hydrothermally altered BQM is also enriched in LREE when chondrite-normalized, which implies that the REE were not strongly fractionated during hydrothermal mineralization.

4.3. REE trends in Berkeley Pit water

Analytical results for REE and other selected trace metals in water from the Berkeley Pit are given in Tables 2 and 3, respectively. REE profiles for pit water (Fig. 4) have been normalized vs. C1 chondrite, vs. NASC, and vs. BQM. When normalized vs. C1 chondrite (Fig. 4a), the Berkeley Pit waters show a general enrichment in the light REE, as well as a positive cerium and negative europium anomaly. When normalized vs. NASC (Fig. 4b), the trend reverses to an enrichment in the middle and heavy REE, the Eu anomaly disappears, and the Ce anomaly is weaker. A similar trend is noted for the pit water vs. BQM diagram (Fig. 4c).

The lack of systematic differences between the Ce concentration of filtered vs. nonfiltered samples (Fig. 5) indicates that cerium in the water column was present primarily in the dissolved phase. Similar

results were obtained for all of the REE, as well as the other trace metals of interest. In this study, the term “dissolved” refers to metal that passes through a 0.45- μm filter, and could include fine colloids with a diameter < 0.45 μm . However, because the REE and U did not partition strongly into filterable particles, it is unlikely that adsorption of these metals onto sub-micron-sized colloidal particles could significantly impact the results and conclusions of this study.

4.4. Variation in REE and other elements with depth

Fig. 6 shows that water from the surface of the Berkeley Pit lake is slightly enriched in REE relative to the deeper water below the thermocline. Exceptions to this trend include samarium and europium, which show very little variation in concentration with depth. The depth profile for cerium is shown in more detail in Fig. 5. The average Ce concentration of all samples

Table 2
Rare-earth element composition of water samples from the Berkeley Pit lake

| Sample | La 139 | Ce 140 | Pr 141 | Nd 146 | Sm 152 | Eu 151 | Gd 157 | Tb 159 | Dy 163 | Ho 165 | Er 168 | Tm 169 | Yb 174 | Lu 175 |
|------------|--------|--------|--------|--------|--------|--------|--------|--------|--------|--------|--------|--------|--------|--------|
| 0.3-FA 284 | 284 | 1132 | 108 | 496 | 121 | 32.4 | 174 | 29.3 | 185 | 39.1 | 113 | 16.4 | 103.4 | 15.6 |
| 0.3-RA 287 | 287 | 1145 | 109 | 502 | 125 | 33.4 | 174 | 28.7 | 183 | 37.8 | 111 | 15.8 | 102.9 | 15.5 |
| 0.9-FA 285 | 285 | 1148 | 109 | 497 | 123 | 32.2 | 170 | 28.7 | 183 | 38.2 | 111 | 16.1 | 102.5 | 15.6 |
| 0.9-RA 286 | 286 | 1150 | 109 | 493 | 124 | 33.2 | 172 | 28.7 | 183 | 38.5 | 111 | 16.1 | 102.0 | 15.8 |
| 1.5-FA 292 | 292 | 1172 | 112 | 510 | 127 | 34.2 | 167 | 28.5 | 186 | 38.2 | 112 | 16.2 | 102.9 | 15.9 |
| 1.5-RA 285 | 285 | 1145 | 108 | 500 | 124 | 33.1 | 168 | 28.0 | 180 | 38.0 | 110 | 15.7 | 100.7 | 15.5 |
| 1.5-RA 289 | 289 | 1154 | 110 | 499 | 125 | 33.4 | 167 | 28.0 | 182 | 37.3 | 110 | 15.8 | 102.0 | 15.6 |
| dup | | | | | | | | | | | | | | |
| 3.0-FA 282 | 282 | 1139 | 109 | 499 | 125 | 33.9 | 165 | 27.7 | 175 | 37.1 | 109 | 15.5 | 103.3 | 15.3 |
| 3.0-RA 286 | 286 | 1147 | 110 | 509 | 128 | 33.9 | 165 | 27.9 | 177 | 37.8 | 109 | 15.5 | 102.1 | 15.4 |
| 9.1-FA 274 | 274 | 1090 | 106 | 500 | 125 | 33.4 | 164 | 27.6 | 178 | 37.4 | 109 | 15.5 | 101.8 | 15.3 |
| 9.1-RA 269 | 269 | 1064 | 105 | 484 | 123 | 32.8 | 161 | 26.8 | 174 | 36.0 | 105 | 14.9 | 99.1 | 15.2 |
| 15-FA 265 | 265 | 1055 | 104 | 484 | 125 | 33.0 | 160 | 27.0 | 174 | 36.3 | 105 | 15.2 | 100.4 | 15.2 |
| 15-RA 270 | 270 | 1072 | 106 | 491 | 123 | 32.7 | 160 | 27.1 | 174 | 37.0 | 106 | 15.2 | 99.8 | 15.1 |
| 30-FA 267 | 267 | 1063 | 104 | 483 | 122 | 32.8 | 159 | 27.7 | 178 | 37.4 | 107 | 15.5 | 101.4 | 15.1 |
| 30-FA 268 | 268 | 1061 | 106 | 487 | 124 | 33.4 | 162 | 27.0 | 174 | 36.2 | 103 | 15.3 | 100.3 | 15.2 |
| dup | | | | | | | | | | | | | | |
| 30-RA 267 | 267 | 1059 | 105 | 483 | 123 | 33.7 | 164 | 26.7 | 174 | 36.4 | 106 | 15.2 | 99.5 | 15.4 |
| 91-FA 267 | 267 | 1066 | 105 | 484 | 123 | 33.3 | 163 | 27.0 | 177 | 36.6 | 106 | 15.4 | 99.5 | 15.4 |
| 91-RA 266 | 266 | 1052 | 105 | 483 | 122 | 33.2 | 163 | 27.2 | 176 | 36.1 | 108 | 15.4 | 98.7 | 15.0 |
| 152-FA 263 | 263 | 1053 | 105 | 489 | 122 | 33.1 | 162 | 27.0 | 176 | 36.2 | 105 | 15.1 | 100.7 | 15.1 |
| 152-RA 270 | 270 | 1055 | 105 | 490 | 122 | 33.2 | 159 | 26.9 | 174 | 36.1 | 105 | 15.2 | 100.3 | 15.1 |
| 210-FA 269 | 269 | 1055 | 104 | 481 | 124 | 33.2 | 160 | 26.9 | 172 | 36.1 | 102 | 15.5 | 100.1 | 15.0 |
| 210-RA 264 | 264 | 1053 | 103 | 483 | 123 | 33.3 | 160 | 27.0 | 172 | 36.0 | 105 | 14.9 | 98.6 | 15.5 |
| Blank | 0.46 | -0.00 | 0.18 | 0.00 | 0.45 | 0.09 | 0.30 | 0.11 | 0.15 | 0.03 | 0.00 | 0.01 | 0.01 | 0.07 |
| IDL | 0.0187 | 0.0135 | 0.0093 | 0.0271 | 0.0161 | 0.0185 | 0.0375 | 0.0074 | 0.0157 | 0.0094 | 0.0221 | 0.0091 | 0.0140 | 0.0086 |

All units are in $\mu\text{g/l}$. Sample prefix is depth (m) of sampling; FA = filtered acidified; RA = raw (nonfiltered) acidified; dup = field duplicate sample; IDL = method detection limit. Blank = deionized water filtered through 0.45- μm filter, into HDPE bottle, with same acid matrix as samples.

Table 3
Concentration of selected additional elements in the Berkeley Pit lake

| Sample | Ba 135 | Sc 45 | Y 89 | Zr 90 | Th 232 | U 238 |
|--------|--------|-------|-------|-------|--------|--------|
| 0.3-FA | 15.3 | 35.6 | 877 | 3.08 | 127 | 826 |
| 0.3-RA | 16.2 | 36.2 | 889 | 2.45 | 127 | 840 |
| 0.9-FA | 16.0 | 32.8 | 871 | 1.94 | 127 | 856 |
| 0.9-RA | 14.0 | 35.1 | 878 | 1.44 | 128 | 852 |
| 1.5-FA | 15.8 | 34.8 | 896 | 1.86 | 130 | 859 |
| 1.5-RA | 15.3 | 34.7 | 877 | 1.74 | 126 | 844 |
| 1.5-RA | 15.4 | 34.4 | 890 | 1.56 | 125 | 839 |
| dup | | | | | | |
| 3.0-FA | 15.6 | 33.5 | 879 | 1.90 | 128 | 838 |
| 3.0-RA | 16.2 | 34.2 | 890 | 1.39 | 129 | 860 |
| 9.1-FA | 12.4 | 33.7 | 879 | 1.47 | 131 | 861 |
| 9.1-RA | 12.2 | 32.5 | 858 | 1.23 | 127 | 843 |
| 15-FA | 12.6 | 34.3 | 864 | 1.49 | 130 | 858 |
| 15-RA | 12.4 | 32.6 | 887 | 1.38 | 130 | 851 |
| 30-FA | 12.3 | 33.6 | 857 | 1.56 | 132 | 880 |
| 30-FA | 12.5 | 33.4 | 876 | 1.67 | 130 | 864 |
| dup | | | | | | |
| 30-RA | 12.8 | 34.5 | 872 | 1.36 | 132 | 870 |
| 91-FA | 11.3 | 33.5 | 871 | 1.69 | 130 | 873 |
| 91-RA | 16.5 | 32.9 | 869 | 1.20 | 131 | 881 |
| 152-FA | 12.6 | 32.1 | 871 | 1.26 | 132 | 882 |
| 152-RA | 12.2 | 33.7 | 872 | 1.44 | 132 | 879 |
| 210-FA | 12.7 | 32.8 | 878 | 1.22 | 132 | 872 |
| 210-RA | 14.7 | 33.3 | 873 | 1.32 | 131 | 883 |
| Blank | 9.8 | 0.0 | 0.00 | 2.95 | 0.13 | 0.00 |
| IDL | 0.06 | 0.16 | 0.001 | 0.014 | 0.0004 | 0.0002 |

All units are in $\mu\text{g/l}$. See notes in Table 2 for more details.

collected in the top 3 m was $1148 \pm 11 \mu\text{g/l}$ (1σ , $n=9$), which compares with $1059 \pm 6 \mu\text{g/l}$ (1σ , $n=11$) for all samples below 10 m depth. This represents an enrichment of 8.4% in the shallow vs. deep water. Taken as a whole, the average enrichment factor for the lanthanide series in shallow vs. deep water was 4.4%, with cerium showing the greatest degree of enrichment above the thermocline, and samarium and europium the least (no significant change between shallow vs. deep water). As for the other elements analyzed, Ba, Sc, and Zr were slightly enriched in shallow vs. deep water, whereas Th and U were depleted (Table 3).

The reasons for why the trace elements of interest were variably enriched or depleted above the thermocline are not completely understood. The most probable explanation for the general trend of REE enrichment towards the surface of the lake is evapoconcentration. In Butte, annual pan evaporation typically exceeds annual precipitation ($\sim 30 \text{ cm}$) by a

factor of roughly 2. As shown by Jonas (2000), the concentration of conservative solutes such as Mg^{2+} tends to increase slightly towards the lake surface. However, evaporation should enrich all elements to an identical degree, and therefore does not explain the

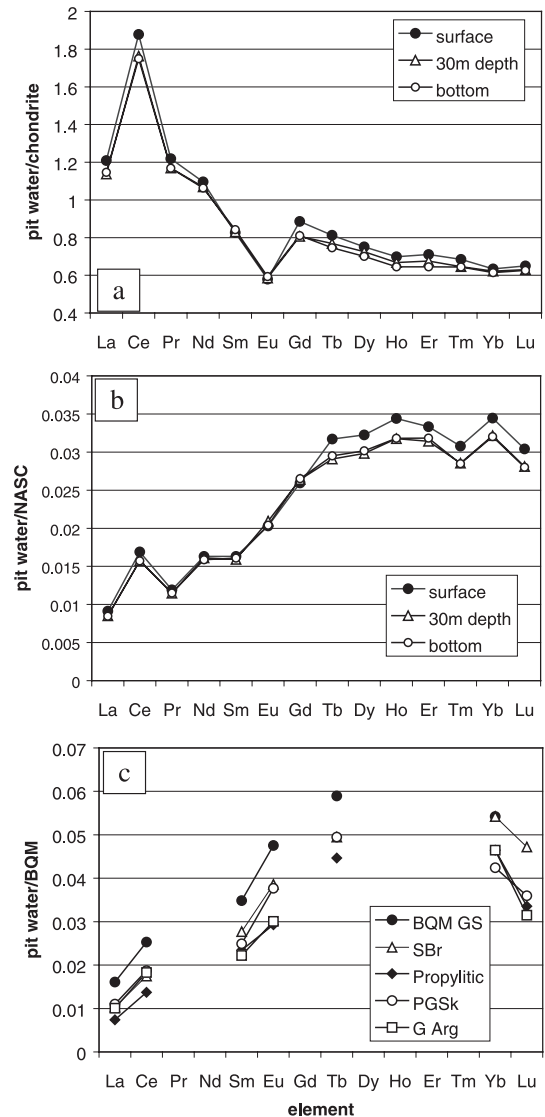


Fig. 4. REE profiles for the Berkeley Pit waters, normalized to: (a) C1 chondrite; (b) NASC; (c) different hydrothermal alteration facies of the BQM. For (a) and (b), data are shown for filtered samples from the surface and bottom of the lake, as well as a depth of 30 m. With the exception of Sm and Eu, most elements show a slight enrichment near the surface. For (c), only data from 30 m depth were used. See caption of Fig. 3 for more information.

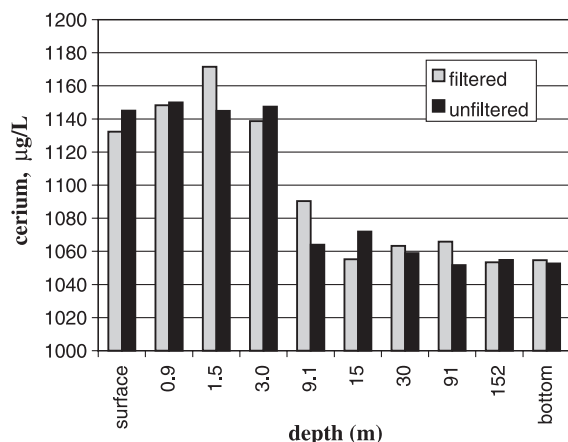


Fig. 5. Filtered vs. nonfiltered concentration of cerium as a function of depth in the Berkeley Pit lake.

differences noted in the preceding paragraph. Given the fact that cerium can exist in the +4 as well as the +3 valence, it is tempting to hypothesize that the larger enrichment of Ce above the thermocline could be due to redox-sensitive reactions. However, thermodynamic calculations (see below) indicate that cerium should exist overwhelmingly in the trivalent state at the pH and Eh conditions of the Berkeley Pit. It is also possible that REE or trace metal fractionation occurs due to adsorption onto secondary precipitates. Judging from turbidity profiles (Fig. 2), solid particles are most abundant at relatively shallow depth above the thermocline. However, it has been previously demonstrated (Fig. 5) that Ce and the other REE are not partitioned strongly into suspended particles. An alternative explanation is that the water chemistry of the shallow pit lake was influenced by mixing with local surface water (i.e., pit wall runoff) during infrequent rain or snowmelt events. It is possible that this water would have a REE and trace element signature that differs from the bulk of the pit lake.

4.5. Partitioning experiments

The results of the partitioning experiments are summarized in Tables 4 and 5, and Fig. 7. The rows labeled “aqueous” and “solid” in Tables 4 and 5 refer to the metal concentrations of the equilibrated water and precipitate fractions, respectively. The rows labeled K_d give the computed distribution coefficients, in units of $(\text{mg/kg})_{\text{solid}}/(\text{mg/l})_{\text{aqueous}}$. These K_d values

are plotted separately in Fig. 8. Overall, no clear differences were found between the results at 15, 30, or 50 days. Based on these results, it is evident that Fe, S, and, to a lesser extent, Ca were the main components in the precipitates that formed during aging of Berkeley Pit water (Table 5). All other elements, including Al, K, Na, Mg, and Si, constituted a very minor percentage (<0.2%) of the total mass. Because Berkeley Pit water is saturated with gypsum (Robins et al., 1997), and since some evaporative loss of water did occur during the experiments, it was assumed that all of the Ca in the solid precipitated as gypsum. Correcting the S mass balance for loss of gypsum, the average atomic ratio of Fe/S in the remaining precipitates was 4.6:1. The natural compound with an Fe/S ratio closest to this value is schwertmannite. According to Bigham et al. (1996), natural schwertmannite has a wide range in composition, with an “average” formula of $\text{Fe}_8\text{O}_8(\text{SO}_4)_{1.25}(\text{OH})_{5.5}$ (Fe/S mole ratio = 6.4:1). The lower Fe/S ratio in the precipitates of this study could be explained by sorption of excess SO_4^{2-} onto the very fine particles as they formed. The presence of schwertmannite in the bench-top oxidation experiments of this study is consistent with previous studies that have identified schwertmannite in suspended solids from the Berkeley Pit lake (Jonas, 2000), as well as water–rock interaction experiments involving Berkeley Pit water (Newbrough and Gammons, 2002). Moreover, Robins

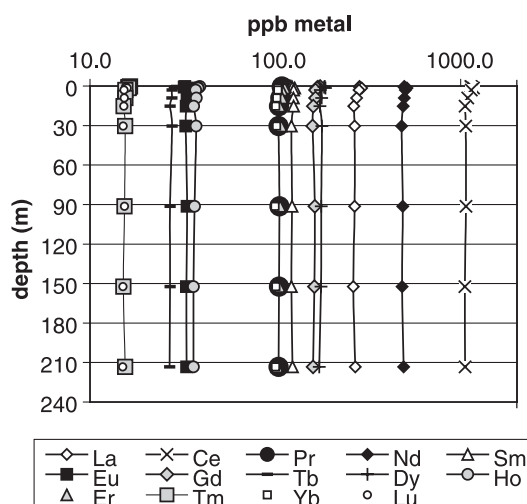


Fig. 6. Filtered REE concentrations vs. depth in the Berkeley Pit lake.

Table 4
Results of partitioning experiments: data for REE

| | La | Ce | Pr | Nd | Sm | Eu | Gd | Tb | Dy | Ho | Er | Tm | Yb | Lu |
|---|------|--------|-------|-------|-------|------|-------|------|------|------|-------|------|------|------|
| <i>Berkeley Pit water initial composition</i> | | | | | | | | | | | | | | |
| Aqueous | 266 | 994 | 104 | 457 | 114 | 31.5 | 170.6 | 26.6 | 174 | 37.0 | 104.1 | 16.4 | 94.3 | 15.4 |
| <i>After 15 days</i> | | | | | | | | | | | | | | |
| Aqueous | 302 | 1137 | 116 | 519 | 130 | 34.2 | 194 | 28.3 | 197 | 40.5 | 116 | 16.7 | 107 | 15.8 |
| Solid | 2289 | 10,908 | 1049 | 5157 | 1132 | 247 | 1034 | 150 | 789 | 135 | 336 | 40.6 | 236 | 30.0 |
| K_d | 7.58 | 9.59 | 9.06 | 9.94 | 8.68 | 7.22 | 5.33 | 5.30 | 4.01 | 3.34 | 2.89 | 2.43 | 2.22 | 1.90 |
| <i>After 30 days</i> | | | | | | | | | | | | | | |
| Aqueous | 306 | 1154 | 118 | 526 | 132 | 34.7 | 198 | 25.5 | 200 | 40.7 | 118 | 16.8 | 107 | 15.9 |
| Solid | 2596 | 12,483 | 1253 | 6038 | 1332 | 279 | 1171 | 165 | 841 | 131 | 324 | 33.9 | 209 | 20.9 |
| K_d | 8.48 | 10.82 | 10.65 | 11.48 | 10.06 | 8.02 | 5.93 | 6.46 | 4.22 | 3.21 | 2.74 | 2.02 | 1.95 | 1.31 |
| <i>After 50 days</i> | | | | | | | | | | | | | | |
| Aqueous | 303 | 1142 | 117 | 523 | 132 | 35.1 | 196 | 25.4 | 198 | 40.7 | 117 | 17.2 | 106 | 16.3 |
| Solid | 2160 | 10,645 | 1027 | 4939 | 1078 | 222 | 950 | 129 | 686 | 100 | 240 | 24.6 | 181 | 15.6 |
| K_d | 7.12 | 9.33 | 8.75 | 9.44 | 8.17 | 6.31 | 4.85 | 5.08 | 3.46 | 2.45 | 2.04 | 1.43 | 1.70 | 0.96 |
| <i>Average K_d values</i> | | | | | | | | | | | | | | |
| K_d (avg.) | 7.73 | 9.91 | 9.49 | 10.28 | 8.97 | 7.19 | 5.37 | 5.61 | 3.89 | 3.00 | 2.56 | 1.96 | 1.96 | 1.39 |

All data are in $\mu\text{g/l}$ (ppb).

et al. (1997) and Gammons et al. (in review) have shown that shallow Berkeley Pit water is supersaturated with schwertmannite.

Relatively few trace metals partitioned strongly into the ferric precipitates (Table 5). For example, the average K_d values for Cu, Mn, and Zn were all below 2. Presumably, the low pH of the Berkeley Pit waters prevented these cationic metals from adsorbing strongly onto the schwertmannite surfaces. In contrast, the distribution coefficients for arsenic and phosphorus were very high (>5000 and 1380, respectively), indicating that these elements partitioned strongly into the precipitates. This is attributed to the anionic forms of dissolved arsenic and phosphorus in oxidized Berkeley Pit water (H_2AsO_4^- and H_2PO_4^-), which—like sulfate—should adsorb strongly onto the positively charged surfaces of freshly precipitated schwertmannite at $\text{pH} < 3$. It is also possible that some phosphate precipitated as the mineral strengite ($\text{FePO}_4 \cdot 2\text{H}_2\text{O}$) (see Discussion). In either case, our results are in agreement with the earlier study of Jonas (2000), who showed that dissolved As and P concentrations in the Berkeley Pit decrease towards the surface of the lake, where ferric precipitates form.

Results for REE from the partitioning experiments are shown in Table 4. The average K_d values for each

lanthanide element are given in the bottom row of Table 4. All of the REE partition weakly ($1 < K_d < 11$) into the solid precipitates, with a trend of increasing and then decreasing K_d across the lanthanide series, peaking at Nd (Fig. 8). Significantly, the experimental trend in K_d across the REE series does not correlate well with the inter-element trends in concentration of REE towards the surface of the Berkeley Pit lake, described in the previous section. For example, in the experiments, cerium partitioned to a greater extent into the ferric precipitates than most of the other REE. However, in the depth profile from the Berkeley Pit lake, cerium showed the greatest increase in dissolved concentration above the thermocline, where precipitates were forming. It seems that partitioning of REE onto secondary solid particles cannot fully explain the differences in REE trends observed between the shallow vs. deep pit lake.

4.6. Aqueous speciation of REE and U in the Berkeley Pit lake

To determine the aqueous speciation of REE in the Berkeley Pit waters, the water analysis collected from a depth of 15 m below surface in May of 1998 (Table 1) was input into the program MINTQA2 (Allison et

Table 5
Results of partitioning experiments: data for selected additional elements

| | Al | As | Ca | Cu | Fe | K | Mg | Mn | Na | P | S | Si | Sr | Th | U | Y | Zn |
|---|------|---------|------|------|-------------------|------|------|-------|------|------|--------|------|------|-------|------|------|------|
| <i>Berkeley Pit water initial composition</i> | | | | | | | | | | | | | | | | | |
| Aqueous | 270 | 0.52 | 425 | 184 | 978 | 5.94 | 444 | 229 | 60.9 | 0.68 | 2661 | 52.0 | 1.19 | 0.116 | 0.77 | 1.04 | 630 |
| <i>After 15 days</i> | | | | | | | | | | | | | | | | | |
| Aqueous | 307 | 0.16 | 478 | 209 | 788 | 6.84 | 507 | 260 | 70.4 | 0.37 | 3020 | 60.7 | 1.33 | 0.132 | 0.91 | 1.21 | 716 |
| Solid | 204 | 699 | 5510 | 368 | 4.5×10^5 | <56 | <250 | <14 | <145 | 501 | 60,600 | <310 | <17 | 1.56 | 0.92 | 3.07 | 274 |
| K_d | 0.66 | 4230 | 11.5 | 1.76 | 574 | <8 | <0.5 | <0.05 | <2 | 1350 | 20.1 | <5 | – | 15.0 | 1.01 | 2.54 | 0.38 |
| <i>After 30 days</i> | | | | | | | | | | | | | | | | | |
| Aqueous | 320 | <0.08 | 485 | 216 | 777 | 7.67 | 509 | 262 | 79.0 | 0.43 | 2980 | 59.9 | 1.36 | 0.135 | 0.93 | 1.24 | 715 |
| Solid | 210 | 703 | 8770 | 384 | 4.6×10^5 | <56 | <250 | 27.1 | <145 | 433 | 63,100 | <310 | 17.3 | 1.51 | 0.62 | 3.06 | 228 |
| K_d | 0.66 | $>10^4$ | 18.1 | 1.78 | 592 | <8 | <0.5 | 0.10 | <2 | 1015 | 21.2 | <5 | 12.8 | 11.6 | 0.66 | 2.46 | 0.32 |
| <i>After 50 days</i> | | | | | | | | | | | | | | | | | |
| Aqueous | 318 | <0.08 | 482 | 214 | 766 | 7.59 | 507 | 261 | 113 | 0.36 | 298 | 60.0 | 1.35 | 0.134 | 0.92 | 1.23 | 711 |
| Solid | 277 | 738 | 9140 | 391 | 4.7×10^5 | <56 | <250 | 64.0 | <145 | 427 | 67,190 | <310 | 16.4 | 1.68 | 0.76 | 2.55 | 500 |
| K_d | 0.87 | $>10^4$ | 19.0 | 1.83 | 610 | <8 | <0.5 | 0.24 | <2 | 1173 | 22.5 | <5 | 12.1 | 11.2 | 0.83 | 2.08 | 0.70 |
| <i>Average K_d values</i> | | | | | | | | | | | | | | | | | |
| K_d (avg.) | 0.73 | $>10^4$ | 16.2 | 1.79 | 592 | <8 | <0.5 | 0.17 | <2 | 1180 | 21.3 | <5 | 12.4 | 12.6 | 0.84 | 2.36 | 0.47 |

All units are in mg/l (ppm).

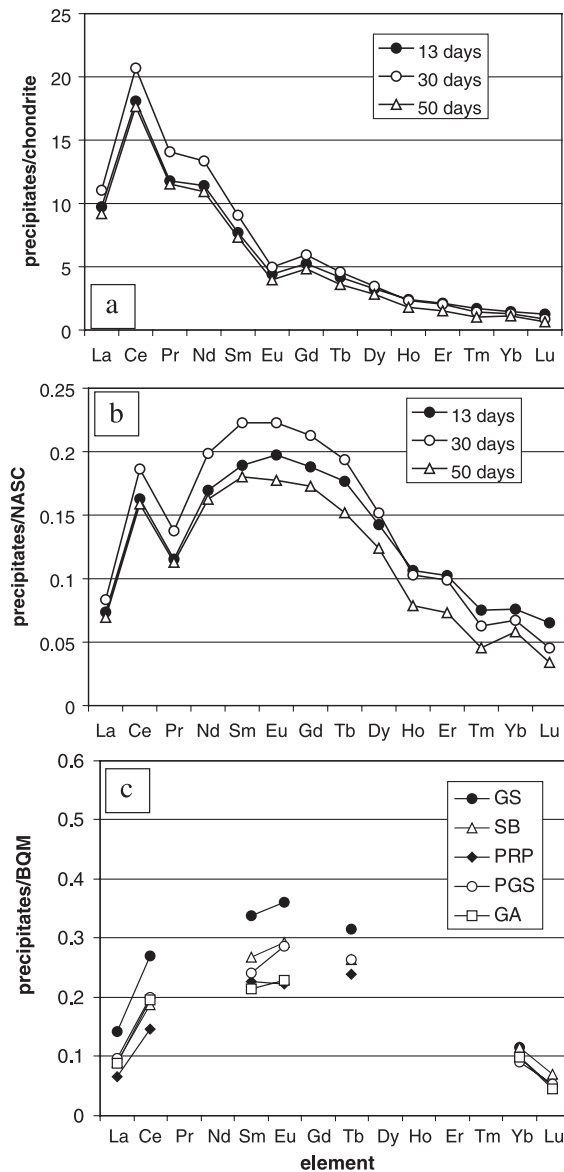


Fig. 7. REE concentration of precipitates formed in bench-top oxidation experiments, normalized to: (a) CI chondrite; (b) NASC shale; (c) hydrothermally altered facies of the Butte Quartz Monzonite. See caption of Fig. 3 for more information.

al., 1991). An aqueous speciation was performed, using the Davies equation for individual ion activity coefficients. (Here and elsewhere in this paper, the standard states adopted were the pure solid at the temperature (T) and pressure (P) of interest, the pure

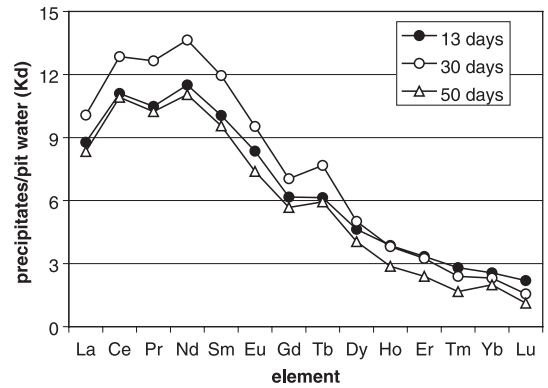


Fig. 8. Variation in K_d for partitioning of REE between ferric precipitates and pit water.

gas at 1 bar pressure and T , and the hypothetically ideal 1-molal solution for aqueous species at T and P .) The calculated concentration and chemical activity of various ligands of interest are summarized in Table 6. The results indicate that sulfate and bisulfate are by far the most abundant ligands in the Berkeley Pit waters, with chloride ion a distant third. The next step in the speciation procedure was to assemble a set of equilibrium constants for formation of aqueous REE complexes with each of the ligands in Table 6. An example set of constants and their sources are listed for cerium in Table 7. The selected equilibrium constants were added to the MINTQA2 database. The results are summarized in Table 7, and show that the majority of total Ce—roughly 87%—is predicted to be ion-paired with sulfate, with the uncomplexed Ce^{3+} ion making up most of the balance. The next

Table 6
Calculated ligand speciation of Berkeley Pit water^a

| Ligand | Molality | Activity | Gamma |
|---------------------------|----------|----------|-------|
| SO_4^{2-} | 4.78e-02 | 1.40e-02 | 0.293 |
| HSO_4^- | 3.06e-03 | 2.25e-03 | 0.736 |
| Cl^- | 3.41e-04 | 2.51e-04 | 0.736 |
| VO_2^+ | 2.47e-06 | 1.82e-06 | 0.736 |
| HCO_3^- | 5.15e-07 | 3.79e-07 | 0.736 |
| H_2PO_4^- | 4.62e-07 | 3.40e-07 | 0.736 |
| F^- | 3.13e-07 | 2.30e-07 | 0.736 |
| HPO_4^{2-} | 2.20e-11 | 6.46e-12 | 0.293 |
| OH^- | 8.73e-13 | 6.42e-13 | 0.736 |
| CO_3^{2-} | 1.22e-14 | 3.58e-15 | 0.293 |
| PO_4^{3-} | 1.02e-20 | 6.46e-22 | 0.063 |

^a Calculated using MINTQA2, $T=4.2$ °C, $I=0.232$, and using the Davies equation for individual ion activity coefficients (gamma).

Table 7
Speciation of cerium in Berkeley Pit water

| Species | log β^a | log β^b | Molal | Activity | Gamma | % of ΣCe |
|--|---------------|---------------|----------|----------|-------|------------------------|
| CeSO ₄ ⁺ | 3.62 | 3.62 | 3.05e–06 | 2.25e–06 | 0.736 | 65.1 |
| Ce(SO ₄) ₂ ⁻ | ~ 5.0 | | 1.03e–06 | 7.56e–07 | 0.736 | 21.9 |
| Ce ³⁺ | | | 6.08e–07 | 3.84e–08 | 0.063 | 13.0 |
| CeF ²⁺ | 3.86 | 4.19 | 4.67e–10 | 1.37e–10 | 0.293 | 9.96e–03 |
| CeCl ²⁺ | 0.47 | 0.31 | 6.72e–11 | 1.97e–11 | 0.293 | 1.43e–03 |
| CeHCO ₃ ²⁺ | 2.42 | 1.95 | 7.61e–12 | 2.23e–12 | 0.293 | 1.62e–04 |
| CeH ₂ PO ₄ ²⁺ | ~ 1.5 | 2.43 | 6.73e–12 | 1.97e–12 | 0.293 | 1.43e–04 |
| Ce(OH) ²⁺ | | 5.59 | 1.76e–13 | 5.16e–14 | 0.293 | 3.75e–06 |
| CeF ₂ ⁺ | 7.3 | 7.27 | 5.15e–14 | 3.79e–14 | 0.736 | 1.10e–06 |
| CeCO ₃ ⁺ | 7.56 | 7.4 | 6.79e–15 | 5.00e–15 | 0.736 | 1.45e–07 |
| CeCl ₂ ⁺ | | 0.31 | 6.71e–15 | 4.94e–15 | 0.736 | 1.43e–07 |
| CeF ₃ (aq) | | 9.52 | 1.47e–18 | 1.55e–18 | 1.055 | 3.14e–11 |
| Ce(OH) ₂ ⁺ | | 11.62 | 2.60e–19 | 1.91e–19 | 0.736 | 5.54e–12 |
| CeCl ₃ (aq) | | -0.36 | 2.51e–19 | 2.65e–19 | 1.055 | 5.36e–12 |
| CeCl ₄ ⁻ | | -0.77 | 3.52e–23 | 2.59e–23 | 0.736 | 7.50e–16 |
| Ce(OH) ₃ (aq) | | 15.85 | 1.06e–26 | 1.12e–26 | 1.055 | 2.26e–19 |
| Ce(OH) ₄ ⁻ | | 17.22 | 1.23e–36 | 9.07e–37 | 0.736 | 2.63e–29 |

The log β values in bold print were used in the speciation calculations. Gamma = activity coefficients, calculated using the Davies equation. The final column gives the percentage of total dissolved Ce of each respective complex.

^a Cumulative formation constants (β) for 25 °C, 1 bar, $I=0.0$, from Wood (1990).

^b Cumulative formation constants (β) for 25 °C, 1 bar, $I=0.0$, Haas et al. (1995).

most abundant species, CeF²⁺, accounted for less than 0.01% of the total. Because the stabilities of the REE–sulfate complexes show very little variation across the

periodic table (Wood, 1990; Haas et al., 1995), very similar speciation results were obtained for the other lanthanide elements.

Table 8
Speciation of uranium in Berkeley Pit water

| Species | log β^a | Molal | Activity | Gamma | % of ΣU |
|---|-------------------|----------|----------|-------|-----------------------|
| UO ₂ (SO ₄) ₂ ⁻ | 4.18 | 1.59e–06 | 4.85e–07 | 0.305 | 39.33 |
| UO ₂ SO ₄ ^o | 3.15 ^b | 1.34e–06 | 1.41e–06 | 1.047 | 33.19 |
| UO ₂ ²⁺ | | 1.10e–06 | 3.36e–07 | 0.305 | 27.19 |
| UO ₂ F ⁺ | 5.11 | 1.12e–08 | 8.34e–09 | 0.743 | 0.28 |
| UO ₂ H ₃ SiO ₄ ⁺ | -2.4 | 1.27e–09 | 9.45e–10 | 0.743 | 3.14e–02 |
| UO ₂ HPO ₄ (aq) | 20.81 | 4.66e–10 | 4.88e–10 | 1.047 | 1.15e–02 |
| UO ₂ OH ⁺ | -5.09 | 3.49e–10 | 2.59e–10 | 0.743 | 8.61e–03 |
| UO ₂ H ₂ PO ₄ ⁺ | 22.64 | 1.56e–10 | 1.16e–10 | 0.743 | 3.86e–03 |
| UO ₂ Cl ⁺ | 0.22 | 1.54e–10 | 1.15e–10 | 0.743 | 3.81e–03 |
| UO ₂ (HPO ₄) ₂ ⁻ | 42.99 | 1.32e–10 | 4.03e–11 | 0.305 | 3.27e–03 |
| UO ₂ CO ₃ (aq) | 10.07 | 1.41e–11 | 1.47e–11 | 1.047 | 3.47e–04 |
| UO ₂ F ₂ (aq) | 8.92 | 1.02e–11 | 1.06e–11 | 1.047 | 2.51e–04 |
| UO ₂ (H ₂ PO ₄) ₂ (aq) | 44.7 | 3.15e–14 | 3.29e–14 | 1.047 | 7.77e–07 |
| (UO ₂) ₂ (OH) ₂ ⁺ | -5.65 | 2.74e–14 | 8.36e–15 | 0.305 | 6.77e–07 |
| UO ₂ F ₃ ⁻ | 11.36 | 7.28e–16 | 5.41e–16 | 0.743 | 1.80e–08 |
| UO ₂ (H ₂ PO ₄) ₃ ⁻ | 66.25 | 3.54e–18 | 2.63e–18 | 0.743 | 8.74e–11 |
| UO ₂ (CO ₃) ₂ ⁻ | 17.01 | 8.82e–19 | 2.69e–19 | 0.305 | 2.18e–11 |
| UO ₂ F ₄ ⁻ | 12.61 | 5.91e–21 | 1.80e–21 | 0.305 | 1.46e–13 |
| (UO ₂) ₃ (OH) ₅ ⁺ | -15.6 | 2.69e–24 | 2.00e–24 | 0.743 | 6.64e–17 |
| UO ₂ (CO ₃) ₃ ⁻ | 21.38 | 1.28e–26 | 1.10e–28 | 0.009 | 3.16e–19 |

See notes in Table 7 for more details.

^a Cumulative formation constants (β) for 25 °C, 1 bar, $I=0.0$. All data are from MINTQA2.

^b Data from Langmuir (1997).

Unlike cerium, a fairly complete set of thermodynamic data exists in the MINTEQ database for U(VI) complexes. In most cases, the stability constants in MINTEQ are similar to the values recommended by Langmuir (1997). The only change we deemed necessary was to increase the log K for $\text{UO}_2\text{SO}_4^\circ$ from 2.71 (MINTEQ) to 3.15 (recommended by Langmuir, 1997). The results of the uranium speciation (Table 8) show very similar results to those for the rare earths, with $\sim 72\%$ of the total U complexed with sulfate, and most of the balance as the uranyl ion, UO_2^{2+} .

The possibility that dissolved Ce and U could exist in other valence states was considered. In the case of Ce, the theoretical Eh of the $\text{Ce}^{4+}/\text{Ce}^{3+}$ boundary was calculated by SUPCRT92 (Johnson et al., 1992) to reside at +1.75 V, well above the stability field of water. Similarly, the activity of U^{4+} was estimated from the measured Eh and pH of the pit waters, and the standard electrical potential for the $\text{U}^{4+}/\text{UO}_2^{2+}$ redox couple from Langmuir (1997). The computed $\text{UO}_2^{2+}/\text{U}^{4+}$ ratio was $>10^{20}$, confirming the overwhelming predominance of U(VI) vs. U(IV) in the pit waters.

5. Discussion

Shale-normalized MREE enrichments appear to be a common feature of acid waters, and have been previously reported by Nordstrom et al. (1995), Gimeno et al. (1996, 2000), Johannesson et al. (1996), Bundy et al. (1996), Leybourne et al. (1998), Elbaz-Poulichet and Dupuy (1999), Johannesson and Zhou (1999), Verplanck et al. (1997, 1998a, 1999), and Worrall and Pearson (2001a). In most of these cases, the pattern observed is one in which the NASC-normalized REE concentrations increase steeply from LREE to MREE, and then decrease more gently from MREE to HREE. In the case of the Berkeley Pit waters, the pattern is similar, except that the profiles are relatively flat from MREE (Tb) to HREE (Lu), when normalized to NASC (Fig. 4b).

A number of hypotheses have been proposed to explain the enrichment in MREE observed in acidic waters. The discussion centers upon whether the REE patterns observed in these waters are inherited from source minerals with similar profiles (“source-controlled”), or are influenced by fractionation during

weathering and transport (“process-controlled”). A number of studies, including our own, have shown that REE in strongly acidic waters dissolve mainly as the free metal ions, or as sulfate ion pairs (Johannesson and Lyons, 1995; Johannesson et al., 1996; Johannesson and Zhou, 1999; this study). Because the stability constants of the Ln-sulfate ion pairs show very little variation across the lanthanide series, aqueous complexation alone should not result in significant REE fractionation in acidic waters.

The fact that the REE signatures of the Berkeley Pit waters differ markedly from those of the Butte Quartz Monzonite (Fig. 4c) would appear, at first glance, to discount the source-controlled hypothesis. However, it is important to realize that each specific REE-bearing mineral in a given rock could have a REE signature that differs from the bulk rock. For example, Bundy et al. (1996) proposed that convex-upward REE trends in effluent mine waters in Colorado are due to selective dissolution of apatite, which itself portrays a convex-upward REE signature when normalized to the host tuff and granite. Although we have bulk REE data for different alteration facies of the Butte Quartz Monzonite, no data exist on REE concentrations or inter-element profiles of individual REE-minerals, such as zircon, apatite, or monazite. For this reason, the hypothesis that the observed REE profiles in the lake waters may be inherited from selective dissolution of a particular source mineral cannot be discounted at this time.

Two processes that could conceivably fractionate REE in the Berkeley Pit lake include sorption onto clays or secondary ferric precipitates, and dissolution or precipitation of secondary minerals enriched in REE. Each of these processes is discussed below.

5.1. Partitioning of REE into secondary precipitates

Gosselin et al. (1992) and Johannesson and Zhou (1999) suggested that MREE enrichments in acidic, natural waters owe their origin to dissolution of secondary Fe–Mn oxy-hydroxide minerals that are similarly enriched in MREE. However, the REE profiles of ferric precipitates formed by ageing of Berkeley Pit water (Fig. 7b) show little resemblance to the REE profile of the NASC-normalized pit waters (Fig. 4b). Thus, it is unlikely that the REE patterns in the pit waters could have formed by dissolution of

ferric precipitates. On the other hand, it is plausible that the patterns could have formed by *precipitation* of these compounds.

Based on the results of our experiments involving ageing of Berkeley Pit water (Fig. 8), it is clear that the LREE are selectively partitioned into the ferric precipitates vs. the MREE and HREE. However, because the magnitude of the distribution coefficients are small (<12), a relatively large mass of ferric precipitate is needed to influence the REE profile of the water. In our bench-top experiments, 200 g of Fe^{2+} -rich pit water produced only about 130 mg of precipitate after oxidation. This corresponds to a water/solid mass ratio of 1540, far too high for the solids formed to affect the REE profile of the water. To examine this further, theoretical REE profiles were generated by equilibrating water with an initially flat NASC-normalized profile with ferric precipitates at different water/rock ratios. In each calculation, lanthanides were partitioned between aqueous and solid phases using the K_d values obtained in this study, while maintaining a closed-system REE mass balance. The results, summarized in Fig. 9, show that selective partitioning of LREE into the ferric precipitates can generate an overall REE profile with a slope similar to that of the Berkeley Pit waters, but only at very low water/solid ratios (<10). Such low water/rock ratios

are impossible when one considers the mass of precipitate that can be generated by a single volume of pit water, but are not inconceivable when one considers the mass of blasted and weathered rock exposed on the submerged mine walls of the pit, as well as the long and tortuous pathway that each aliquot of groundwater must follow before it reaches the Berkeley Pit lake. Because several cubic kilometers of bedrock were dewatered during underground and open pit mining at Butte, secondary ferric precipitates likely formed and are now present in much of the flooded fractures and mine openings surrounding the Berkeley Pit. No data are available at this time on the REE concentration of these groundwaters.

Verplanck et al. (1999) recently conducted experiments very similar to ours, in which unpreserved mine waters from the Western U.S. were allowed to oxidize for 6 months. It was found that REE were enriched in the precipitates in all samples, but that the magnitude of this enrichment increased steeply with increase in pH. For example, for mine waters with $\text{pH} < 2$, REE were approximately 10 times higher in the precipitate vs. the aqueous phase. This ratio increased to $\sim 50:1$ for $\text{pH} 2.5\text{--}3$, and $\sim 3000:1$ for $\text{pH} 4.2$. Consistent with our study, Verplanck et al. (1999) found that partitioning of REE into the solids had little or no effect on the REE concentration of the residual fluids, since only a small fraction of the total REE originally in solution was removed. Unlike our study, Verplanck et al. reported no clear trends in K_d of REE with atomic number.

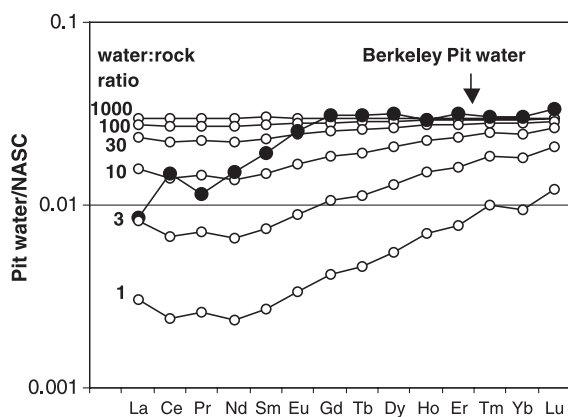


Fig. 9. Theoretical REE profiles generated by equilibrating water with ferric precipitates at different water/rock ratios (ranging from 1 to 1000). The NASC-normalized REE profile of the starting solution was arbitrarily set at a slope of 0. The lanthanides were then partitioned into the solids, using K_d values obtained in this study. The actual NASC-normalized REE pattern of Berkeley Pit water is shown for comparison.

5.2. Solubility controls on aqueous concentrations of REE and U

Given the high levels of REE and U in the Berkeley Pit waters, we examined the possibility that the concentrations of these elements might be constrained by equilibrium solubility reactions. The saturation index (SI) is defined as follows:

$$\text{SI} = \log Q/K \quad (2)$$

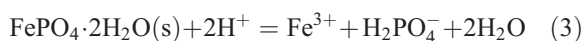
where Q is the observed or measured ion activity quotient, and K is the equilibrium constant for the solubility controlling reaction. A positive value of SI indicates supersaturated conditions, whereas a negative value indicates undersaturation.

In the case of the REE, oxides and hydroxides of the form Ln_2O_3 and $\text{Ln}(\text{OH})_3$ were strongly undersaturated, as were the REE-sulfates and REE-carbonates. Solubility products for these calculations were taken from Smith and Martell (1976), Rard (1988), Firsching and Brune (1991a), and Wood et al. (2002). In contrast, the hydrous REE-phosphates (rhabdophane) were somewhat closer to saturation. Rhabdophane is a common weathering product of REE-rich apatite (Banfield and Eggleton, 1989). The solubility of synthetic REE-phosphate has been investigated by Firsching and Brune (1991b) and Byrne and Kim (1993). Using their data, we calculated saturation indices for REE-phosphates in Berkeley Pit water at 15.2 m depth. Table 9 shows that saturation indices for all of the hydrous REE-phosphates generally range between -3 and -6 , indicating a relatively high degree of undersaturation. It should be noted that these calculations have considerable uncertainty, as they hinge greatly on the accuracy of the estimated activity of free phosphate ion (PO_4^{3-}), as well as the free lanthanide ions (Ln^{3+}). Nonetheless, it is unlikely that the combined uncertainties in the thermodynamic modeling could offset the low SI values obtained.

Another phase that could potentially be limiting REE mobility in the Berkeley Pit lake is REE-rich crandallite (a.k.a. florencite). Crandallite minerals have a crystal structure similar to alunite, with the

general formula $\text{AB}_3(\text{XO}_4)_2(\text{OH})_6 \cdot \text{H}$ (Schwab et al., 1990). The A site is typically filled with Ca, the B site by Al or Fe^{3+} , and the X site by P or As. Trivalent lanthanides can substitute for $(\text{Ca}^{2+} + \text{H}^+)$. Crandallites strongly enriched in REE are known to form, along with rhabdophane, during chemical weathering of apatite or monazite-rich protoliths. They have been reported in laterites and ferricretes (Angelica and da Costa, 1991; Schwab et al., 2000), and reportedly are “highly insoluble”. However, using thermodynamic data in Schwab et al. (1993), Berkeley pit waters were shown to be highly undersaturated with Ce-crandallite ($\text{SI} = -20$), indicating that this phase should not be present in the flooded pit.

It is also possible that REE concentrations in the pit waters could be limited by co-precipitation with Fe-phosphate (strengite). Previous workers have proposed that Fe-phosphate compounds could play a key role in controlling REE concentrations in rivers (Sholkovitz, 1995; Johannesson et al., 1995). Although strengite has not been directly observed in studies of the Berkeley Pit lake, its presence may be inferred from geochemical modeling of the pit waters. Published K_{sp} 's for the following reaction:



range from -5.61 to -7.65 (Vieillard and Tardy, 1984). The most careful study appears to be that of Nriagu (1972), who obtained $\log K_{\text{sp}} = -6.85$, which is also the value entered into the MINTEQA2 database. Using the data of Nriagu (1972), our calculated SI values for strengite range from $+1.5$ in the shallow pit lake, to $+1.0$ at depth (see Fig. 10). Considering the various sources of analytical and modeling errors, it appears likely that strengite is exerting a solubility control on phosphate concentrations in the Berkeley Pit lake. The calculated SI values are higher in the shallow waters, because of the higher $\text{Fe}^{3+}/\text{Fe}^{2+}$ ratio near the surface of the lake (Fig. 10). Precipitation of strengite could explain the slight decrease in total P for the shallow vs. deep pit waters (Fig. 10). If so, then it is possible that some REE could co-precipitate with strengite as a REE-phosphate compound.

Saturation indices for possible U(VI) and U(IV) solids were calculated using a spreadsheet, with

Table 9

Solubility products (K_{sp}), ion activity products (IAP), and saturation indices (SI) for $\text{LnPO}_4 \cdot n\text{H}_2\text{O}$ minerals

| Element | $\log K_{\text{sp}}$ | | Berkeley Pit water | | |
|---------|----------------------|--------|--------------------|---------|---------|
| | FB91 | BK93 | $\log \text{IAP}$ | SI-FB91 | SI-BK93 |
| La | -25.44 | | -28.99 | -3.55 | |
| Ce | | -24.26 | -28.40 | | -4.14 |
| Pr | -25.4 | | -29.41 | -4.01 | |
| Nd | -25.42 | | -28.75 | -3.33 | |
| Sm | -25.31 | | -29.35 | -4.04 | |
| Eu | -25.06 | -24.24 | -29.94 | -4.88 | -5.7 |
| Gd | -24.69 | -24.13 | -29.27 | -4.58 | -5.14 |
| Tb | -24.36 | | -30.04 | -5.68 | |
| Dy | -24.41 | | -29.24 | -4.83 | |
| Ho | -25.35 | | -29.93 | -4.58 | |
| Er | -25.07 | | -29.48 | -4.41 | |
| Tm | -25.41 | | -30.32 | -4.91 | |
| Yb | -25.53 | -23.34 | -29.51 | -3.98 | -6.17 |
| Lu | -24.7 | | -30.33 | -5.63 | |

FB91 = Firsching and Brune (1991a,b); BK93 = Byrne and Kim (1993).

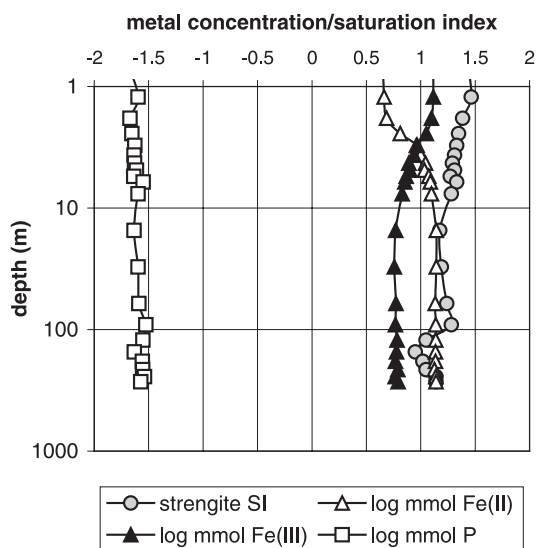


Fig. 10. Variation in the concentration of Fe^{2+} , Fe^{3+} and P, and changes in the saturation index of strengite, with depth in the Berkeley Pit lake.

solubility products taken from Langmuir (1997) and Vieillard and Tardy (1984), and the preliminary aqueous speciation computed using MINTeq, as described in the preceding section. The results, summarized in Table 10, suggest that all of the uranium-

bearing phases examined are undersaturated in the Berkeley Pit lake. The mineral closest to saturation is tyuyamunite ($\text{Ca}(\text{UO}_2)_2(\text{VO}_4)_2$), with an SI value of -3.11 . Although the low saturation index would appear to preclude the existence of this phase, the SI value is extremely sensitive to the measured pH, as shown by the stoichiometry of the solubility controlling reaction (Table 10). For the water sample of interest, a rise in pH of only 0.5 log units was sufficient to theoretically supersaturate the pit water with tyuyamunite. It is possible that substitution of other divalent cations—such as Fe, Mg, Cu, or Zn—into the Ca site could further stabilize this phase. Thus, the possibility that the concentration of uranium in the pit lake may be solubility-controlled cannot be entirely dismissed.

An alternate hypothesis is that UO_2^{2+} behaves conservatively, and that its concentration is simply a function of the rate of input from weathering and wall-rock leaching compared to the total water flux. However, unlike most elements that were evapo-concentrated, U was one of the few solutes that showed a significant decrease in concentration in the topmost portion of the water column (Table 2). This suggests that the behavior of U is not entirely conservative. Adsorption onto secondary ferric precipitates or clays,

Table 10
Saturation indices for various uranium minerals in Berkeley Pit water

| Mineral name | Solubility reaction | $\log K_{sp}$ | SI | Source |
|---------------|--|---------------|----------|--------|
| Tyuyamunite | $\text{Ca}(\text{UO}_2)_2(\text{VO}_4)_2(\text{s}) + 8\text{H}^+ = \text{Ca}^{2+} + 2\text{UO}_2^{2+} + 2\text{VO}_2^+ + 4\text{H}_2\text{O}$ | -3.56 | -3.11 | 1 |
| | $\text{Cu}(\text{UO}_2)_2(\text{PO}_4)_2 \cdot 8\text{H}_2\text{O}(\text{s}) + 4\text{H}^+ = \text{Cu}^{2+} + 2\text{UO}_2^{2+} + 2\text{H}_2\text{PO}_4^- + 3\text{H}_2\text{O}$ | -12.8 | -5.13 | 2 |
| H-autunite | $\text{UO}_2\text{HPO}_4 \cdot 4\text{H}_2\text{O}(\text{s}) + 2\text{H}^+ = \text{UO}_2^{2+} + \text{H}_3\text{PO}_4(\text{aq}) + 4\text{H}_2\text{O}$ | -2.5 | -6.04 | 1 |
| | $\text{UO}_2\text{HPO}_4(\text{s}) + \text{H}^+ = \text{UO}_2^{2+} + \text{H}_2\text{PO}_4^-$ | -3.48 | -6.40 | 2 |
| Rutherfordine | $\text{UO}_2\text{CO}_3(\text{s}) = \text{UO}_2^{2+} + \text{CO}_3^{2-}$ | -14.49 | -6.43 | 1 |
| | $\text{UO}_2\text{HPO}_4 \cdot 4\text{H}_2\text{O}(\text{s}) + \text{H}^+ = \text{UO}_2^{2+} + \text{H}_2\text{PO}_4^- + 4\text{H}_2\text{O}$ | -3.42 | -6.46 | 2 |
| Schoepite | $\text{UO}_3 \cdot 2\text{H}_2\text{O}(\text{s}) + 2\text{H}^+ = \text{UO}_2^{2+} + 3\text{H}_2\text{O}$ | 5.20 | -6.59 | 1 |
| | $\text{KUO}_2\text{PO}_4(\text{s}) + 2\text{H}^+ = \text{K}^+ + \text{UO}_2^{2+} + \text{H}_2\text{PO}_4^-$ | -3.55 | -7.58 | 2 |
| | $\text{H}_2(\text{UO}_2)_2(\text{PO}_4)_2 \cdot 10\text{H}_2\text{O}(\text{s}) + 2\text{H}^+ = 2\text{UO}_2^{2+} + 2\text{H}_3\text{PO}_4^- + 10\text{H}_2\text{O}$ | -11.85 | -7.91 | 2 |
| Bassetite | $\text{Fe}(\text{UO}_2)_2(\text{PO}_4)_2(\text{s}) + 6\text{H}^+ = \text{Fe}^{2+} + 2\text{UO}_2^{2+} + 2\text{H}_3\text{PO}_4(\text{aq})$ | -3.73 | -10.82 | 3 |
| Soddyite | $(\text{UO}_2)_2\text{SiO}_4 \cdot 2\text{H}_2\text{O}(\text{s}) + 4\text{H}^+ = 2\text{UO}_2^{2+} + \text{H}_4\text{SiO}_4(\text{aq}) + 2\text{H}_2\text{O}$ | 5.74 | -11.21 | 1 |
| Carnotite | $\text{K}_2(\text{UO}_2)_2(\text{VO}_4)_2(\text{s}) + 8\text{H}^+ = 2\text{K}^+ + 2\text{UO}_2^{2+} + 2\text{VO}_2^+ + 4\text{H}_2\text{O}$ | 0.56 | -12.40 | 1 |
| | $(\text{UO}_2)_3(\text{PO}_4)_2 \cdot 4\text{H}_2\text{O}(\text{s}) + 6\text{H}^+ = 3\text{UO}_2^{2+} + 2\text{H}_3\text{PO}_4(\text{aq}) + 4\text{H}_2\text{O}$ | -6 | -12.47 | 1 |
| Uraninite | $\text{UO}_2(\text{s}) + 4\text{H}^+ = \text{U}^{4+} + 2\text{H}_2\text{O}$ | -4.99 | -12.87 | 1 |
| Autunite | $\text{Ca}(\text{UO}_2)_2(\text{PO}_4)_2(\text{s}) = \text{Ca}^{2+} + 2\text{UO}_2^{2+} + 2\text{PO}_4^{3-}$ | -44.7 | -13.31 | 1 |
| Torbernite | $\text{Cu}(\text{UO}_2)_2(\text{PO}_4)_2(\text{s}) + 6\text{H}^+ = \text{Cu}^{2+} + 2\text{UO}_2^{2+} + 2\text{H}_3\text{PO}_4(\text{aq})$ | -1.82 | -13.43 | 3 |
| | $(\text{UO}_2)_3(\text{PO}_4)_2(\text{s}) + 4\text{H}^+ = 3\text{UO}_2^{2+} + 2\text{H}_2\text{PO}_4^-$ | -7.2 | -13.95 | 2 |
| Uranophane | $\text{Ca}(\text{H}_3\text{O})_2(\text{UO}_2)_2(\text{SiO}_4)_2 \cdot 3\text{H}_2\text{O}(\text{s}) + 6\text{H}^+ = \text{Ca}^{2+} + 2\text{H}_4\text{SiO}_4(\text{aq}) + 2\text{UO}_2^{2+} + 5\text{H}_2\text{O}$ | 9.42 | -15.11 | 1 |
| Na-weeksite | $\text{Na}_2(\text{UO}_2)_2(\text{Si}_2\text{O}_5)_3 \cdot 4\text{H}_2\text{O}(\text{s}) + 6\text{H}^+ + 5\text{H}_2\text{O} = 2\text{Na}^+ + 2\text{UO}_2^{2+} + 6\text{H}_4\text{SiO}_4(\text{aq})$ | 1.5 | -20.30 | 1 |
| Coffinite | $\text{USiO}_4(\text{am}) + 4\text{H}^+ = \text{U}^{4+} + \text{H}_4\text{SiO}_4(\text{aq})$ | 0.5 | -21.05 | 1 |

Source: 1 = Langmuir (1997); 2 = Vieillard and Tardy (1984); 3 = calculated from data in Langmuir (1997).

or co-precipitation with a phosphate mineral—such as strengite—are two processes that could serve to limit U mobility below the controls of saturation with a pure U-bearing solid phase.

6. Conclusions

This study has explored various aspects of the aqueous geochemistry of REE and U in the acidic Berkeley Pit lake, and how these elements partition between the water column and secondary precipitates forming in the lake. Like many acidic waters, REE patterns in the Berkeley Pit are depleted in LREE when normalized to shale. However, a complimentary depletion in HREE relative to MREE is not shown. The depletion in LREE could be due to partitioning of these elements onto the surfaces of secondary precipitates forming in the lake, or onto similar secondary phases in the fractured and weathered bedrock surrounding the lake. This hypothesis is broadly consistent with the trend in distribution coefficients (K_d) vs. atomic number obtained in bench-top experiments. However, the REE profiles differ in detail. Also, because the magnitude of the K_d values is small, pit water must equilibrate with a very large mass of ferric precipitate for the latter to have an influence on the REE profiles of the aqueous phase. Although the aqueous concentrations of REE and U do not appear to be limited by solubility controls, we do not discount the possible importance of solid solutions, or phases for which thermodynamic data are not presently available. If such compounds are present, and if their solubility products vary across the lanthanide series, then this could possibly explain the observed REE fractionation trends in the Berkeley Pit lake. It is clear that more work is needed before the fate and transport of REE in the Berkeley Pit lake, as well as in other acidic waters in general, are completely understood.

Acknowledgements

This project would not have been possible without the cooperation of the Montana Bureau of Mines and Geology and Montana Resources, in collecting samples. We are also grateful to William M. Shannon

for his expert analysis of the samples for REE, Mark Reed for generously providing the REE data for the Butte Quartz Monzonite, Amber Henne for assistance with the bench-top oxidation experiments, and the late Bill Chatham for analytical assistance during Jim Jonas' thesis work. The manuscript was improved by the thoughtful reviews of R.N. Tempel, W.B. Lyons, and E.H. Oelkers. [EO]

References

- Allison, J.D., Brown, D.S., Novo-Gradac, K.J., 1991. MINTEQA2/PRODEFA2, A Geochemical Assessment Model for Environmental Systems. U.S. Environmental Protection Agency, Athens, GA. EPA/600/3-91/021.
- Anders, E., Grevesse, N., 1989. Abundances of the elements; meteoritic and solar. *Geochim. Cosmochim. Acta* 53, 197–214.
- Angelica, R.S., da Costa, M.L., 1991. Geochemistry of rare-earth elements in surface lateritic rocks and soils from the Maicuru Complex, Para, Brazil. *J. Geochem. Explor.* 47, 165–182.
- Åström, M., 2001. Abundance and fractionation patterns of rare earth elements in streams affected by acid sulphate soils. *Chem. Geol.* 175, 249–258.
- Banfield, J.F., Eggleton, R.A., 1989. Apatite replacement and rare earth mobilization, fractionation, and fixation during weathering. *Clays Clay Miner.* 37, 113–127.
- Bigham, J.M., Schwertmann, U., Traina, S.J., Winland, R.L., Wolf, M., 1996. Schwertmannite and the chemical modeling of iron in acid sulfate waters. *Geochim. Cosmochim. Acta* 60, 2111–2121.
- Bundy, M.E., Oreskes, N., Hanchar, J.M., 1996. Origin of convex-upward REE trends in bog seep and mine effluent waters in Paradise Basin, San Juan Mountains, CO. *Abstr. Programs - Geol. Soc. Am.* 28, A-469.
- Byrne, R.H., Kim, K.H., 1993. Rare earth precipitation and coprecipitation behavior: the limiting role of PO_4^{3-} on dissolved rare earth concentrations in seawater. *Geochim. Cosmochim. Acta* 57, 519–526.
- Carlson-Foszcz, V.L., Oreskes, N., Nordstrom, D.K., 1991. Mobility of rare earth elements in the Ophir region, San Juan Mountains, Colorado. *EOS Trans. - Am. Geophys. Union* 72, 308.
- Davis, A., Ashenberg, D., 1989. The aqueous geochemistry of the Berkeley Pit, Butte, Montana, USA. *Appl. Geochem.* 44, 23–36.
- Duaime, T.E., Metesh, J.J., Kerschen, M.D., Dunstan, C.B., 1998. The flooding of Butte's underground mines and Berkeley Pit: 15 years of water-level monitoring (1982–1997). *Montana Bur. Mines Geol., Open File Report*, vol. 376. 116 pp.
- Elbaz-Poulichet, F., Dupuy, C., 1999. Behaviour of rare earth elements at the freshwater–seawater interface of two acid mine rivers: the Tinto and Odiel (Andalucia, Spain). *Appl. Geochem.* 14, 1063–1072.
- Firsching, F.H., Brune, S.N., 1991a. Solubility products of the trivalent rare earth phosphates. *J. Chem. Eng. Data* 36, 93–95.

- Firsching, F.H., Brune, S.N., 1991b. Solubility products of the rare-earth carbonates. *J. Chem. Eng. Data* 31, 40–42.
- Gammons, C.H., Poulson, S., Madison, J.P., Jonas, J.P., in review. Iron cycling and subaqueous pyrite oxidation in the flooded Berkeley Pit, Montana.
- German, C.R., Masuzawa, T., Greaves, M.J., Elderfield, H., Edmond, J.M., 1995. Dissolved rare earth elements in the Southern Ocean: cerium oxidation and the influence of hydrography. *Geochim. Cosmochim. Acta* 59, 1551–1558.
- Ghazi, A.M., Roedder, E., Vanko, D.A., 1994. Rare earth elements (REE) in fluid inclusions from the Butte Cu–Mo deposit; an application of flow injection ICP-MS. *Proc. Fifth Biennial Pan-American Conference of Research on Fluid Inclusions*, pp. 22–23.
- Gimeno, M.J., Auque, L.F., Nordstrom, D.K., Bruno, J., 1996. Rare earth element (REE) geochemistry and the tetrad effect in the naturally acidic waters of Arroyo del Val, northeastern Spain. *Abstr. Programs - Geol. Soc. Am.* 28 (7), 468.
- Gimeno, M.J., Auqué, L.F., Nordstrom, D.K., 2000. REE speciation in low-temperature acidic waters and the competitive effects of aluminum. *Chem. Geol.* 165, 167–180.
- Gosselin, D.C., Smith, M.R., Lepel, E.A., Lau, L.J.C., 1992. Rare earth elements in chloride-rich groundwater, Palo Duro Basin, Texas, USA. *Geochim. Cosmochim. Acta* 56, 1495–1505.
- Gromet, L.P., Dymek, R.F., Haskin, L.A., Korotev, R.L., 1984. The “North American shale composite”; its compilation, major and trace element characteristics. *Geochim. Cosmochim. Acta* 48, 2469–2482.
- Haas, J.R., Shock, E.L., Sassani, D.C., 1995. Rare earth elements in hydrothermal systems; estimates of standard partial molal thermodynamic properties of aqueous complexes of the rare earth elements at high pressures and temperatures. *Geochim. Cosmochim. Acta* 59, 4329–4350.
- Hollings, P., Hendry, M.J., Kerrich, R., 1999. Sequential filtration of surface and ground waters from the Rabbit Lake uranium mine, northern Saskatchewan, Canada. *Water Qual. Res. J. Can.* 34, 221–247.
- Johannesson, K.H., Hendry, M.J., 2000. Rare earth element geochemistry of groundwaters from a thick till and clay-rich aquitard sequence, Saskatchewan, Canada. *Geochim. Cosmochim. Acta* 64, 1493–1509.
- Johannesson, K.H., Lyons, W.B., 1994. The rare earth element geochemistry of Mono Lake water and the importance of carbonate complexing. *Limnol. Oceanogr.* 39, 1141–1154.
- Johannesson, K.H., Lyons, W.B., 1995. Rare-earth element geochemistry of Colour Lake, and acidic freshwater lake on Axel Heiberg Island, Northwest Territories, Canada. *Chem. Geol.* 119, 209–223.
- Johannesson, K.H., Zhou, X., 1999. Origin of middle rare earth element enrichments in acid waters of a Canadian High Arctic lake. *Geochim. Cosmochim. Acta* 63, 153–165.
- Johannesson, K.H., Lyons, W.B., Stetzenbach, K.J., Byrne, R.H., 1995. The solubility control of rare earth elements in natural terrestrial waters and the significance of PO_4^{3-} and CO_3^{2-} in limiting dissolved rare earth concentrations; a review of recent information. *Aquat. Geochem.* 1, 157–173.
- Johannesson, K.H., Lyons, W.B., Yelken, M.A., Gaudette, H.E., Stetzenbach, K.J., 1996. Geochemistry of rare earth elements in hypersaline and dilute acidic natural terrestrial waters: complexation behavior and middle rare-earth element enrichments. *Chem. Geol.* 133, 125–144.
- Johnson, J.W., Oelkers, E.H., Helgeson, H.C., 1992. SUPCRT92: a software package for calculating the standard molal thermodynamic properties of minerals, gases, aqueous species, and reactions from 1–5000 bars and 0–1000 °C. *Comput. Geosci.* 18, 899–947.
- Jonas, J.P., 2000. Current seasonal limnology of the Berkeley Pit Lake. *Proc. Fifth Intl. Conf. Acid Rock Drainage. Society of Mining, Metallurgy, and Exploration (SME)*, Littleton, CO, pp. 359–366.
- Langmuir, D., 1997. *Aqueous Environmental Geochemistry*. Prentice-Hall, Upper Saddle River, New Jersey. 600 pp.
- Leybourne, M.I., Goodfellow, W.D., Boyle, D.R., 1998. Hydrogeochemical, isotopic, and rare earth element evidence for contrasting water–rock interactions at two undisturbed Zn–Pb massive sulphide deposits, Bathurst Mining Camp, N.B., Canada. *J. Geochem. Explor.* 64, 237–261.
- Leybourne, M.I., Goodfellow, W.D., Boyle, D.R., Hall, G.M., 2000. Rapid development of negative Ce anomalies in surface waters and contrasting REE patterns in groundwaters associated with Zn–Pb massive sulphide deposits. *Appl. Geochem.* 15, 695–723.
- Metesh, J.J., Duaiame, T.E., 2000. The flooding of Butte’s underground mines and the Berkeley Pit: 18 years of water-quality monitoring (1982–1999). *Montana Bur. Mines Geol., Open File*, vol. 409. 79 pp.
- Meyer, C., Shea, E.P., Goddard Jr., C.C., Zeihen, L.B., Guilbert, J.M., Miller, R.N., McAleer, J.F., Brox, G.B., Ingersoll Jr., R.G., Burns, G.J., Wigal, T., 1968. Ore deposits at Butte, Montana. In: Ridge, J.D. (Ed.), *Ore Deposits of the United States, 1933–1967: The Graton-Sales Volume*. American Inst. Mining, Metall., Petrol. Engineers, New York, pp. 1373–1416.
- Miekeley, N., Couthino de Jesus, H., Porto da Silveira, C.L., Linsalata, P., Morse, R., 1992. Rare-earth elements in groundwaters from the Osamu Utsumi mine and Morro do Ferro analogue study sites, Poços de Caldas, Brazil. *J. Geochem. Explor.* 45, 365–387.
- Miller, R.N. (Ed.), 1973. *Guidebook for the Butte Field Meeting of the Society of Economic Geologists, Butte, Montana*. The Anaconda Company, Butte, MT, August 18–21, 1973.
- Newbrough, P., Gammons, C.H., 2002. Experimental investigation of water–rock interaction and acid mine drainage at Butte, Montana. *Environ. Geol.* 41, 705–719.
- Nordstrom, D.K., Carlson-Foszcz, V., Oreskes, N., 1995. Rare earth element (REE) fractionation during acidic weathering of San Juan Tuff, Colorado. *Abstr. Programs - Geol. Soc. Am.* 27, A-199.
- Nriagu, J.O., 1972. Solubility equilibrium constant of strengite. *Am. J. Sci.* 272, 476–484.
- Pearce, N.J.G., White, R., Fuge, R., 1998. Behaviour of rare earth elements and heavy metals in ochreous mine drainage: analogue elements for the behaviour of the trans-uranic metals. *Abstr. Programs - Geol. Soc. Am.* 30 (7), 128.
- Rard, J.A., 1988. Aqueous solubilities of praseodymium, europium, and lutetium sulfates. *J. Solution Chem.* 17, 499–517.

- Robins, R.G., Berg, R.B., Dysinger, D.K., Duaiame, T.E., Metesh, J.J., Diebold, F.E., Twidwell, L.G., Mitman, G.G., Chatham, W.H., Huang, H.H., Young, C.A., 1997. Chemical, physical and biological interaction at the Berkeley Pit, Butte, Montana. Proceedings, Tailings and Mine Waste '97. Balkema Press, Rotterdam, pp. 521–541.
- Schwab, R.G., Herold, H., Götz, C., de Oliveira, N.P., 1990. Compounds of the crandallite type: synthesis and properties of pure rare earth element-phosphates. *Neues Jahrb. Mineral., Monatsh.* 1990 (6), 241–254.
- Schwab, R.G., Goetz, C., Herold, H., Pinto-de-Oliveira, N., 1993. Compounds of the crandallite type; thermodynamic properties of Ca-, Sr-, Ba-, Pb-, La-, Ce- to Gd-phosphates and -arsenates. *Neues Jahrb. Mineral., Monatsh.* 1993 (12), 551–568.
- Schwab, R.G., Pimpl, T.H., Schukow, H., Breiting, D.K., 2000. Compounds of the crandallite type; material from the Earth on its way to technical application. *Dixue Qianyuan (Earth Sci. Front.)* 7 (2), 485–497.
- Sholkovitz, E.R., 1992. Chemical evolution of rare earth elements: fractionation between colloidal and solution phases of filtered river water. *Earth Planet. Sci. Lett.* 114, 77–84.
- Sholkovitz, E.R., 1995. The aquatic chemistry of rare earth elements in rivers and estuaries. *Aquat. Geochem.* 1, 1–34.
- Sholkovitz, E.R., Schneider, D.L., 1991. Cerium redox cycles and rare earth elements in the Sargasso Sea. *Geochim. Cosmochim. Acta* 55, 2737–2743.
- Smith, R.M., Martell, A.E., 1976. *Critical Stability Constants: Vol. 4. Inorganic Complexes*. Plenum, New York.
- Verplanck, P.L., Nordstrom, D.K., Taylor, H.E., Wright, W.G., 1997. Nonconservative nature of rare earth elements in an acidic alpine stream, upper Animas River basin, Colorado. *Abstr. Programs - Geol. Soc. Am.* 29 (6), 152.
- Verplanck, P.L., Nordstrom, D.K., Taylor, H.E., 1998a. Partitioning of rare earth elements between colloids and acid waters. *Abstr. Programs - Geol. Soc. Am.* 30 (7), 254.
- Verplanck, P.L., Nordstrom, D.K., Wright, W.G., Taylor, H.E., 1998b. Rare earth element geochemistry of acid waters; preliminary results identifying source signatures and instream processes. In: Nimick, D.A., von-Guerard, P. (Eds.), *Science for Watershed Decisions on Abandoned Mine Lands; Review of Preliminary Results*. U.S. Geol. Surv., Open File, vol. 98-0297. 21 pp.
- Verplanck, P.L., Nordstrom, D.K., Taylor, H.E., 1999. Overview of rare earth element investigations in acid waters of U.S. Geological Survey abandoned mine lands watersheds. U.S. Geol. Survey, Water-Resources Investigations Report, vol. 99-4018A, pp. 83–92.
- Vieillard, P., Tardy, Y., 1984. Thermochemical properties of phosphates. In: Nriagu, J.O., Moore, P.B. (Eds.), *Phosphate Minerals*. Springer-Verlag, New York, pp. 199–214.
- Webb, C., Davis, A.D., Hodge, V.F., 1993. Geochemical characterization of acidic waters from uranium mines in the Black Hills of South Dakota. *Abstr. Programs - Geol. Soc. Am.* 25, 323.
- White, R.A., Pearce, N.J.G., Fuge, R., 1998. Behavior of rare earth elements and other metals in synthetic and natural acid mine drainage, a laboratory story. *Abstr. Programs - Geol. Soc. Am.* 30 (7), 254.
- Wood, S.A., 1990. The aqueous geochemistry of the rare-earth elements and yttrium: 1. Review of available low-temperature data for inorganic complexes and the inorganic REE speciation of natural waters. *Chem. Geol.* 82, 159–186.
- Wood, S.A., Palmer, D.A., Wesolowski, D.J., Bénézech, P., 2002. The aqueous geochemistry of the rare earth elements and yttrium: Part XI. The solubility of Nd(OH)₃ and hydrolysis of Nd³⁺ from 30 to 290 °C at saturated water vapor pressure with in-situ pH_m measurement. In: Hellmann, R., Wood, S.A. (Eds.), *Water–Rock Interactions, Ore Deposits, and Environmental Geochemistry: A Tribute to David A. Crerar*. *Geochim. Soc. Special Publication*, vol. 7, pp. 229–256.
- Wood, S.A., Shannon, W.M., Baker, L.L., in press. The aqueous geochemistry of the rare earth elements and yttrium: Part 13. REE geochemistry of mine drainage from the Pine Creek area, Coeur d'Alene River valley, Idaho, USA. In: Johannesson, K.H., (Ed.), *Rare Earth Elements in Groundwater Flow Systems*. Kluwer Academic Publishing.
- Worrall, F., Pearson, D.G., 2001a. The development of acidic groundwater in coal-bearing strata: Part 1. Rare earth element fingerprinting. *Appl. Geochem.* 16, 1465–1480.
- Worrall, F., Pearson, D.G., 2001b. Water–rock interaction in an acidic mine discharge as indicated by rare earth element patterns. *Geochim. Cosmochim. Acta* 65, 3027–3040.